

1 **Pluripotency and the origin of animal multicellularity**

2

3 Shunsuke Sogabe\*<sup>1†</sup>, William L. Hatleberg\*<sup>1†</sup>, Kevin M. Kocot<sup>2</sup>, Tahsha E. Say<sup>1</sup>, Daniel

4 Stoupin<sup>1†</sup>, Kathrein E. Roper<sup>1†</sup>, Selene L. Fernandez-Valverde<sup>1†</sup>, Sandie M. Degnan<sup>1#</sup> and

5 Bernard M. Degnan<sup>1#</sup>

6

7 1. School of Biological Sciences, University of Queensland, Brisbane QLD 4072, Australia

8 2. Department of Biological Sciences and Alabama Museum of Natural History, The

9 University of Alabama, Tuscaloosa, AL 35487 USA

10

11 \* These authors contributed equally to this work

12 # Corresponding authors

13

14 †Present addresses: The Scottish Oceans Institute, Gatty Marine Laboratory, School of

15 Biology, University of St Andrews, East Sands, St Andrews, Fife KY16 8LB, UK (S.S.);

16 Department of Biological Sciences, Carnegie Mellon University, 4400 Fifth Avenue,

17 Pittsburgh, PA 15213 USA (W.L.H.); BioQuest Studios, PO Box 603, Port Douglas

18 QLD 4877, Australia (D.S.); Centre for Clinical Research, Faculty of Medicine, University

19 of Queensland, Herston QLD 4029, Australia (K.R.); CONACYT, Unidad de Genómica

20 Avanzada, Laboratorio Nacional de Genómica para la Biodiversidad, Centro de

21 Investigación y de Estudios Avanzados del IPN, Irapuato, Guanajuato, Mexico (S.L.F.-V.).

22 **The most widely held, but rarely tested, hypothesis for the origin of animals is**  
23 **that they evolved from a unicellular ancestor with an apical cilium surrounded by**  
24 **a microvillar collar that structurally resembled present-day sponge choanocytes**  
25 **and choanoflagellates<sup>1-4</sup>. Here we test this traditional view of the origin of the**  
26 **animal kingdom by comparing the transcriptomes, fates and behaviours of the**  
27 **three primary sponge cell types – choanocytes, pluripotent mesenchymal**  
28 **archeocytes and epithelial pinacocytes – with choanoflagellates and other**  
29 **unicellular holozoans. Unexpectedly, we find the transcriptome of sponge**  
30 **choanocytes is the least similar to the transcriptomes of choanoflagellates and is**  
31 **significantly enriched in genes unique to either animals or to sponges alone. In**  
32 **contrast, pluripotent archeocytes upregulate genes controlling cell proliferation**  
33 **and gene expression, as in other metazoan stem cells and in the proliferating**  
34 **stages of two closely-related unicellular holozoans, including a colonial**  
35 **choanoflagellate. In the context of the body plan of the sponge, *Amphimedon***  
36 ***queenslandica*, we show that choanocytes appear late in development and are the**  
37 **result of a transdifferentiation event. They exist in a metastable state and readily**  
38 **transdifferentiate into archeocytes, which can differentiate into a range of other**  
39 **cell types. These sponge cell type conversions are similar to the temporal cell**  
40 **state changes that occur in many unicellular holozoans<sup>5</sup>. Together, these analyses**  
41 **offer no support for the homology of sponge choanocytes and choanoflagellates,**  
42 **nor for the view that the first multicellular animals were simple balls of cells with**  
43 **limited capacity to differentiate. Instead, our results are consistent with the first**  
44 **animal cell being able to transition between multiple states in a manner similar**  
45 **to modern transdifferentiating and stem cells.**

46 **Main**

47 The last common ancestor of all living animals appears to have possessed epithelial and  
48 mesenchymal cell types that could transdifferentiate over an ontogenetic life cycle  
49 (Fig. 1a)<sup>1,4</sup>. This capacity to develop and differentiate required a regulatory capacity to  
50 control spatial and temporal gene expression, and included a diversified set of signalling  
51 pathways, transcription factors, enhancers, promoters and non-coding RNAs (Fig. 1a)<sup>5-9</sup>.  
52 Recent analyses of the genomes and life cycles of unicellular holozoan relatives of  
53 animals have revealed that the regulatory repertoire present in multicellular animals  
54 largely evolved first in a unicellular ancestor (Fig. 1a)<sup>2,5,6</sup>. These insights contrast with a  
55 widely-held view that all animals evolved from a stem organism that was a simple ball  
56 of ciliated cells<sup>1,3,4</sup>. Implicit in this traditional perspective is that (i) regulatory systems  
57 necessary for cell differentiation evolved after the divergence of metazoan and  
58 choanoflagellates lineages, and (ii) morphological features shared between  
59 choanoflagellate and choanocytes are homologous and were present in the original  
60 animal cell. While the former is not supported by recent data – unicellular holozoans  
61 can change cell states by environmentally-induced temporal shifts in gene expression  
62 (Fig. 1a)<sup>5,6,10-12</sup> – the latter is contingent upon the still controversial aspect of whether  
63 extant choanocytes and choanoflagellates accurately reflect the ancestral animal cell  
64 type.

65 To test this, we first compared cell type-specific transcriptomes<sup>13</sup> from the sponge  
66 *Amphimedon queenslandica* with each other, and with transcriptomes expressed during  
67 the life cycles of closely-related unicellular holozoans, the choanoflagellate *Salpingoeca*  
68 *rosetta*, the filasterean *Capsaspora owczarzaki* and the ichthyosporean *Creolimax*  
69 *fragrantissima* (Fig. 1a)<sup>10-12</sup>. We chose three sponge somatic cell types hypothesised to  
70 be homologous to cells present in the last common ancestor of contemporary

71 metazoans, choanozoans or holozoans: (i) choanocytes, which are internal epithelial  
72 feeding cells that capture food by pumping water through the sponge; (ii) epithelial cells  
73 called pinacocytes, which line internal canals and the outside of the sponge; and (iii)  
74 mesenchymal pluripotent stem cells called archeocytes, which inhabit the middle  
75 collagenous layer and have a range of other functions (Fig. 1 and Supplementary Video  
76 1)<sup>2,14-16</sup>. These three cell types were manually picked and frozen within 15 minutes of *A.*  
77 *queenslandica* being dissociated (see Methods and Supplementary Video 2). Their  
78 transcriptomes were sequenced using CEL-Seq<sup>2</sup><sup>17</sup> and mapped to the Aqu2.1 annotated  
79 genome<sup>18</sup>. This approach allowed visual verification of the three cell types, minimised  
80 the time for transcriptional changes to occur after cell dissociation, and allowed for  
81 deep sequencing of cell type transcriptomes (Extended Data Table 1, and  
82 Supplementary Files S1 and S2).

83 Principle component analysis (PCA) and sparse partial least squares discriminant  
84 analysis (sPLS-DA)<sup>19</sup> reveal that the transcriptomes of the three *A. queenslandica* cell  
85 types are unique, with choanocytes being the most distinct (Fig. 2a and Extended Data  
86 Fig. 1). Of 44,719 protein-coding genes, 11,013 genes were identified as significantly  
87 differentially expressed in at least one cell type from pairwise comparisons between the  
88 three cell types using DESeq<sup>2</sup><sup>20</sup> (Fig. 2b and Supplementary File S3). Significant  
89 differences between cell types were independently corroborated by sPLS-DA, which  
90 highlighted a subset of 110 genes that explain 15% of the variance in the dataset and  
91 clearly discriminate the choanocytes from the other two cell types (Extended Data Fig.  
92 1). This subset includes numerous putative immunity genes that typically encode  
93 multiple domains in unique configurations, including scavenger receptor cysteine-rich,  
94 tetratricopeptide repeat and epidermal growth factor domains (Supplementary File S4).

95 From the DESeq2 analysis, we find that archeocytes significantly upregulate genes  
96 involved in the control of cell proliferation, transcription and translation, consistent  
97 with their function as pluripotent stem cells (Fig. 2c and Supplementary File S5). In  
98 contrast, choanocyte and pinacocyte transcriptomes are enriched in suites of genes  
99 involved in cell adhesion, signalling and polarity, consistent with their role as epithelial  
100 cells (Fig. 2d; Extended Data Figure 2 and Supplementary File S5).

101 We identified the evolutionary age of all protein coding genes in the *Amphimedon*  
102 genome as well as the genes significantly and uniquely up-regulated in each cell-type  
103 specific transcriptome using phylostratigraphy, which is based on sequence similarity  
104 with genes in other organisms with a defined phylogenetic distance<sup>21</sup>. Specifically, we  
105 classified *Amphimedon* genes as having evolved (i) before or (ii) after divergence of  
106 metazoan and choanoflagellate lineages (these are called pre-metazoan and metazoan  
107 genes, respectively), or (iii) after divergence of the sponge lineage from all other  
108 animals (sponge-specific genes). In total, the *A. queenslandica* genome is comprised of  
109 28% pre-metazoan, 26% metazoan and 46% sponge-specific protein-coding genes (Fig.  
110 3a and Supplementary File S6). We find that 43% of genes significantly up-regulated in  
111 choanocytes have homologues detectable only in sponges, which is similar to the entire  
112 genome (Fig. 3b). In contrast, 62% of genes significantly up-regulated in the pluripotent  
113 archeocytes belong to the evolutionarily oldest pre-metazoan category, which is  
114 significantly higher than 28% for the entire genome (Fig. 3c). As with archeocytes,  
115 pinacocytes express significantly more pre-metazoan and fewer sponge-specific genes  
116 than would be expected from the whole genome profile (Fig. 3d). Results supporting  
117 this analysis are obtained when we (i) undertake the same phylostratigraphic analysis  
118 of all genes expressed in these cell types, taking also into account relative transcript  
119 abundances (Extended Data Fig. 3 and Supplementary File S7), or (ii) classify gene age

120 using an alternative method to identify of orthogroups (homology cluster containing  
121 both orthologues and paralogues)<sup>22</sup> among unicellular holozoan, yeast and *Arabidopsis*  
122 coding sequences (Extended Data Fig. 4).

123 Comparison of *A. queenslandica* cell-type transcriptomes with stage-specific  
124 transcriptomes from the choanoflagellate *S. rosetta*<sup>10</sup>, the filasterean *C. owczarzaki*<sup>11</sup> and  
125 the ichthyosporean *C. fragrantissima*<sup>12</sup> reveals that archeocytes have a significantly  
126 similar transcriptome to the colonial stage of the choanoflagellate and the multinucleate  
127 stage of the ichthyosporean (Fig. 3e). Consistent with this result, the significantly up-  
128 regulated genes in the colonial or multinucleate stages of all three unicellular holozoans  
129 share the highest proportion of orthogroups with genes significantly up-regulated in  
130 archeocytes (Extended Data Fig. 5). In contrast, choanocyte and pinacocyte  
131 transcriptomes have no significant similarity to any known unicellular holozoan  
132 transcriptome, and share a lower proportion of orthogroups with unicellular holozoans  
133 compared to archeocytes (Fig. 3e and Extended Data Fig. 5a).

134 When we compare the 94 differentially up-regulated transcription factor genes in *A.*  
135 *queenslandica* choanocytes, pinacocytes and archeocytes, we find no marked difference  
136 in their phylostratigraphic age, suggesting that the gene regulatory networks  
137 operational in these cells are of an overall similar evolutionary age (Extended Data Fig.  
138 6 and Supplementary File S8). We detected 20, 25 and 21 orthologues of the 43  
139 evolutionarily-oldest (i.e. pre-metazoan) transcription factor genes expressed in the  
140 *Amphimedon* cells in the genomes of *Salpingoeca*, *Capsaspora* and *Creolimax*  
141 respectively, with 9 of these being present in all species (Supplementary File S8).  
142 Comparison of the expression profiles of the transcription factor genes shared among  
143 these unicellular holozoans and *Amphimedon* revealed no evidence of a conserved, co-  
144 expressed gene regulatory network (Extended Data Fig. 7 and Supplementary File S8).

145 However, the proto-oncogene *Myc* and its heterodimeric partner *Max* are up-regulated  
146 in *A. queenslandica* archeocytes (Extended Data Fig. 6), as observed in other metazoan  
147 self-renewing pluripotent stem cells<sup>23</sup>. *Myc* and *Max* are present also in  
148 choanoflagellates, filastereans and ichthyosporeans, where they heterodimerise and  
149 bind to E-boxes just as they do in animals<sup>10-12,24</sup>. *Myc* is expressed in the proliferative  
150 stage of *Capsaspora*, where it regulates genes associated with ribosome biogenesis and  
151 translation<sup>6</sup>. Sponge archeocytes also have enriched expression of genes involved in  
152 translation, transcription and DNA replication (Fig. 2c). This suggests that *Myc*'s role in  
153 regulating proliferation and differentiation predates its role in bilaterian stem cells and  
154 cancer<sup>23,25</sup>, and was likely a cardinal feature of the first metazoan cell.

155 Given that we found no transcriptional support for homology of *A. queenslandica*  
156 choanocytes and choanoflagellates, but did find evidence for pluripotent archeocytes  
157 expressing a largely premetazoan transcriptome, we sought to investigate the  
158 relationships of these cell types in the context of development and the body plan. In  
159 *Amphimedon* and most other sponges, archeocytes form during embryogenesis to  
160 populate the inner cell mass of the larva and are the most prevalent cell type during  
161 early metamorphosis<sup>15</sup>. As metamorphosis progresses, these archeocytes differentiate  
162 into other cell types that populate the juvenile body plan, including choanocytes and  
163 pinacocytes, the former of which can transdifferentiate into other cell types<sup>16,26</sup>. To  
164 further understand the stability of choanocytes and the dynamics of  
165 transdifferentiation, we selectively labelled choanocytes in 3 day old juvenile *A.*  
166 *queenslandica* with CM-DiI (Fig. 4a) and followed their fate over 24 hours (Fig. 4b).  
167 Within 4 hours of labelling, many choanocytes dedifferentiated into archeocytes (Fig.  
168 4c, d, Supplementary Video 3); this did not require prior cell division (Extended Data  
169 Fig. 8). By as little as two hours later, some of these CM-DiI labelled archeocytes had

170 differentiated into pinacocytes (Fig. 4e); within 12 hours, we detected multiple labelled  
171 cell types (Fig. 4e, f). Together, these results suggest that archeocytes are essential in  
172 the development and maintenance of the *A. queenslandica* body plan, as appears to be  
173 the case in other sponges<sup>15</sup>. Unlike archeocytes, choanocytes appear late in  
174 development and exist in a metastable state, sometimes lasting only a few hours before  
175 dedifferentiating back into archeocytes (Fig. 4g, Extended Data Fig. 8).

176 In conclusion, our analysis of sponge and unicellular holozoan cell transcriptomes,  
177 development and behaviour provides no support for the long-standing and widely-held  
178 hypothesis that multicellular animals evolved from an ancestor that was an  
179 undifferentiated ball of cells resembling extant choanocytes and choanoflagellates<sup>1-4</sup>.  
180 This conclusion is corroborated by recent studies that question the homology of  
181 choanocytes and choanoflagellates based on cell structure<sup>27,28</sup>. As an alternative, we  
182 posit that the ancestral metazoan cell type, regardless of its external character, had the  
183 capacity to exist in, and transition between, multiple cell states in a manner similar to  
184 modern transdifferentiating and stem cells. Previous analyses of holozoan genomes  
185 support this postulate, with some of the genomic foundations of pluripotency being  
186 established deep in a unicellular past<sup>6,24</sup>. Genomic innovations unique to metazoans,  
187 including the origin and expansion of key signalling pathway and transcription factor  
188 families, and regulatory DNA and RNA classes<sup>7,9,29</sup>, may have conferred the ability of this  
189 ancestral pluripotent cell to evolve a regulatory system where it could co-exist in  
190 multiple states of differentiation, giving rise to the first multicellular animal.

191

192 **References (Main Text)**



- 193 1 Cavalier-Smith, T. Origin of animal multicellularity: precursors, causes,  
194 consequences - the choanoflagellate/sponge transition, neurogenesis and the  
195 Cambrian explosion. *Philos. Trans. R. Soc. Lond. B Biol. Sci.* **372**, 20150476 (2017).
- 196 2 Brunet, T. & King, N. The origin of animal multicellularity and cell differentiation.  
197 *Dev. Cell* **43**, 124-140 (2017).
- 198 3 Arendt, D., Benito-Gutierrez, E., Brunet, T. & Marlow, H. Gastric pouches and the  
199 mucociliary sole: setting the stage for nervous system evolution. *Philos. Trans. R.*  
200 *Soc. Lond. B Biol. Sci.* **370**, 20150286 (2015).
- 201 4 Nielsen, C. Six major steps in animal evolution: are we derived sponge larvae? *Evol.*  
202 *Dev.* **10**, 241-257 (2008).
- 203 5 Sebe-Pedros, A., Degnan, B. M. & Ruiz-Trillo, I. The origin of Metazoa: a unicellular  
204 perspective. *Nat. Rev. Genet.* **18**, 498-512 (2017).
- 205 6 Sebe-Pedros, A. *et al.* The dynamic regulatory genome of *Capsaspora* and the origin  
206 of animal multicellularity. *Cell* **165**, 1224-1237 (2016).
- 207 7 Gaiti, F. *et al.* Landscape of histone modifications in a sponge reveals the origin of  
208 animal *cis*-regulatory complexity. *eLife* **6**, e22194 (2017).
- 209 8 Gaiti, F., Calcino, A. D., Tanurdzic, M. & Degnan, B. M. Origin and evolution of the  
210 metazoan non-coding regulatory genome. *Dev. Biol.* **427**, 193-202 (2017).
- 211 9 Babonis, L. S. & Martindale, M. Q. Phylogenetic evidence for the modular evolution  
212 of metazoan signalling pathways. *Philos. Trans. R. Soc. Lond. B Biol. Sci.* **372**,  
213 20150477 (2016).
- 214 10 Fairclough, S. R. *et al.* Premetazoan genome evolution and the regulation of cell  
215 differentiation in the choanoflagellate *Salpingoeca rosetta*. *Genome Biol.* **14**, R15  
216 (2013).

- 217 11 Sebé-Pedrós, A. *et al.* Regulated aggregative multicellularity in a close unicellular  
218 relative of Metazoa. *eLife* **2**, e01287 (2013).
- 219 12 de Mendoza, A., Suga, H., Permanyer, J., Irimia, M. & Ruiz-Trillo, I. Complex  
220 transcriptional regulation and independent evolution of fungal-like traits in a  
221 relative of animals. *eLife* **4**, e08904 (2015).
- 222 13 Arendt, D. *et al.* The origin and evolution of cell types. *Nat. Rev. Genet.* **17**, 744-757  
223 (2016).
- 224 14 Maldonado, M. Choanoflagellates, choanocytes, and animal multicellularity. *Invert.*  
225 *Biol.* **123**, 1-22 (2004).
- 226 15 Ereskovsky, A. *The Comparative Embryology of Sponges*. Springer, Netherlands  
227 (2010).
- 228 16 Nakanishi, N., Sogabe, S. & Degnan, B. Evolutionary origin of gastrulation: insights  
229 from sponge development. *BMC Biol.* **12**, 26 (2014).
- 230 17 Hashimshony, T. *et al.* CEL-Seq2: sensitive highly-multiplexed single-cell RNA-Seq.  
231 *Genome Biol.* **17**, 77 (2016).
- 232 18 Fernandez-Valverde, S. L., Calcino, A. D. & Degnan, B. M. Deep developmental  
233 transcriptome sequencing uncovers numerous new genes and enhances gene  
234 annotation in the sponge *Amphimedon queenslandica*. *BMC Genom.* **16**, 387 (2015).
- 235 19 Le Cao, K. A., Boitard, S. & Besse, P. Sparse PLS discriminant analysis: biologically  
236 relevant feature selection and graphical displays for multiclass problems. *BMC*  
237 *Bioinform.* **12**, 253 (2011).
- 238 20 Love, M. I., Huber, W. & Anders, S. Moderated estimation of fold change and  
239 dispersion for RNA-seq data with DESeq2. *Genome Biol.* **15**, 1-21 (2014).
- 240 21 Domazet-Lošo, T. & Tautz, D. A phylogenetically based transcriptome age index  
241 mirrors ontogenetic divergence patterns. *Nature* **468**, 815-818 (2010).

- 242 22 Li, L., Stoeckert, C. J. & Roos, D. S. OrthoMCL: identification of ortholog groups for  
243 eukaryotic genomes. *Genome Res.* **13**, 2178-2189 (2003).
- 244 23 Fagnocchi, L. & Zippo, A. Multiple roles of MYC in integrating regulatory networks of  
245 pluripotent stem cells. *Front. Cell Dev. Biol.* **5**, 7 (2017).
- 246 24 Young, S. L., Diolaiti, D., Conacci-Sorrell, M., Ruiz-Trillo, I., Eisenman, R. N. & King, N.  
247 Premetazoan ancestry of the Myc–Max network. *Mol. Biol. Evol.* **28**, 2961–2971  
248 (2011).
- 249 25 Kress, T. R., Sabo, A. & Amati, B. MYC: connecting selective transcriptional control to  
250 global RNA production. *Nat. Rev. Cancer* **15**, 593-607 (2015).
- 251 26 Sogabe, S., Nakanishi, N. & Degnan, B. M. The ontogeny of choanocyte chambers  
252 during metamorphosis in the demosponge *Amphimedon queenslandica*. *EvoDevo* **7**,  
253 6 (2016).
- 254 27 Mah, J. L., Christensen-Dalsgaard, K. K., & Leys, S. P. Choanoflagellate and  
255 choanocyte collar-flagellar systems and the assumption of homology. *Evol. Dev.* **16**,  
256 25–37 (2014).
- 257 28 Pozdnyakov, I., Sokolova, A., Ereskovsky, A., & Karpov, S. Kinetid structure of  
258 choanoflagellates and choanocytes of sponges does not support their close  
259 relationship. *Protistology* **11**, 248-264 (2017).
- 260 29 Srivastava, M. *et al.* The *Amphimedon queenslandica* genome and the evolution of  
261 animal complexity. *Nature* **466**, 720–726 (2010).

262

263 **Supplementary Information** is linked to the online version of the paper at  
264 [www.nature.com/nature](http://www.nature.com/nature). (This submission includes eight Supplementary Information  
265 data files as well as additional material that is available on Dryad.)

266

267 **Acknowledgements**

268 This study was supported by funds from the Australian Research Council (B.M.D. and  
269 S.M.D.). We thank Iñaki Ruiz Trillo for primary expression data for *Capsaspora* and  
270 *Creolimax*.

271

272 **Author Contributions**

273 B.M.D and S.M.D conceived and designed the project. S.S., D.S. and K.R. identified and  
274 isolated the cells, and prepared the libraries. W.H., S.S and K.M.K. undertook gene  
275 expression and annotation, and phylostratigraphic analyses with help from T.S., S.M.D,  
276 S. F.-V and B.M.D. S.S. undertook cell lineage analyses. B.M.D, S.M.D and S.S. wrote the  
277 manuscript with comments and contributions from all authors.

278

279 **Author Information**

280 **Data deposition statement**

281 *Amphimedon queenslandica* genome sequence can be accessed at

282 ([http://metazoa.ensembl.org/Amphimedon\\_queenslandica/Info/Index](http://metazoa.ensembl.org/Amphimedon_queenslandica/Info/Index)).

283 All cell-type transcriptome data are available in the NCBI SRA database under the

284 BioProject PRJNA412708. Additional supplementary data is available upon request

285

286

287

288

289

290 **Competing financial interests**

291 The authors declare no competing financial interests.

292

293 **Corresponding author**

294 Correspondence and requests for materials should be addressed to

295 b.degnan@uq.edu.au or s.degnan@uq.edu.au.

296

297 **Figures Legends**

298

299 **Figure 1. Holozoan relationships and sponge cell types.**

300 **a**, Cellular and regulatory traits of metazoans and closely related unicellular holozoans.

301 Black dots, trait present; white dots, trait absent; grey dots, trait present but to a lesser

302 extent. Two major evolutionary events are mapped onto the holozoan phylogenetic

303 tree: (i) environmentally-induced, facultative changes in cell state ancestral to

304 holozoans; and (ii) obligate metazoan multicellularity. **b**, Whole mount internal view of

305 a juvenile *Amphimedon queenslandica*. Cell types are outlined. A, archeocyte (cluster of

306 four outlined); Cc, choanocyte chamber; S, sclerocyte; Sp, spherulous cell; P, pinacocyte.

307 **c**, Choanocyte chamber labelled with DiI with an illustration of a single choanocyte

308 below. **d**, Pinacocyte labelled with DiI with illustration below. **e**, Archeocyte labelled

309 with DiI with illustration below. Scale bars: b, 10  $\mu$ m; c-e, 5  $\mu$ m.

310

311 **Figure 2. Comparison of choanocyte, archeocyte and pinacocyte transcriptomes.**

312 **a**, PCA plot of CEL-Seq2 transcriptomes with 95% confidence level ellipse plots. Blue,

313 choanocytes; red, archeocytes; green, pinacocytes. **b**, Venn diagram summary of the

314 number of significantly up-regulated genes based on pairwise comparisons between

315 each of the three cell types using DESeq2 with a false discovery rate (FDR) < 0.05. The

316 percentages are of the total genes differentially up-regulated in all cell types. **c**,

317 Percentage of KEGG Genetic Information Processing genes present in each cell type,  
318 corresponding to the number of components making up each KEGG category identified.  
319 **d**, Heat map of the expression of *Amphimedon* epithelial cell polarity, junction and basal  
320 lamina genes in each cell type.

321

322 **Figure 3. Analysis of gene age of choanocyte, archeocyte and pinacocyte**  
323 **transcriptomes.**

324 **a**, Phylostratigraphic estimate of the evolutionary age of coding genes in the *A.*  
325 *queenslandica* genome. **b-d**, Estimate of gene age of differentially-expressed genes in  
326 choanocytes (b), archeocytes (c) and pinacocytes (d) and the enrichment of phylostrata  
327 relative to the whole genome (bottom). Asterisks indicate significant difference (p-value  
328 <0.001) from the whole genome. **e**, A heat map comparing orthologous genes uniquely  
329 up-regulated in *A. queenslandica* cell types, and *Salpingoeca rosetta*, *Capsaspora*  
330 *owczarzaki* and *Creolimax fragrantissima* life cycle stages. Colour indicates the  
331 significance of overlap based on the odds ratio. Values indicate adjusted p-values and  
332 show significant resemblance only between the archeocyte and the *S. rosetta* colonial  
333 stage and the *C. fragrantissima* multinucleate stage. N.s., not significant.

334

335 **Figure 4. Transdifferentiation of choanocytes in *Amphimedon queenslandica*.**

336 **a, b**, Whole mount views of 4 day old juveniles labelled with CM-DiI. **a**, 30 min after CM-  
337 DiI labelling. Labelling is almost exclusively in choanocytes in chambers; insert, a single  
338 labelled choanocyte chamber. **b**, 24 hours after labelling. CM-DiI labelling spread  
339 throughout the juvenile with limited staining still present in choanocyte chambers;  
340 insert, a choanocyte chamber comprising largely of unlabelled cells. **c, d**, 2 hours (c) and  
341 4 hours (d) after labelling. Labelled cells (arrow) migrating outside of choanocyte

342 chambers (dotted lines), some of which have a large nucleus and a clearly visible  
343 nucleolus (arrowheads) characteristic of archeocytes. **e**, 6 hours after initial DiI  
344 labelling of choanocytes, labelled pinacocytes (arrow) with thin pseudopodia are  
345 detected. **f**, 12 hours after initial labelling, CM-DiI labelled skeletal sclerocytes (arrow)  
346 and other cell types are present. **g**, Summary diagram of cell type transition in the *A.*  
347 *queenslandica* juvenile. Scale bars: a, b, 200  $\mu\text{m}$ ; c-f, 10  $\mu\text{m}$ .

348

349

## 350 **Methods**

351

### 352 **Cell isolation**

353 Adult *Amphimedon queenslandica* were collected from Heron Island Reef, Great Barrier  
354 Reef and transferred to a closed aquarium facility where they were housed for no more  
355 than three days before being cut into approximately 1 cm<sup>3</sup> cubes. These cubes were  
356 mechanically dissociated by squeezing through a 20  $\mu\text{m}$  mesh. The resultant cell  
357 suspension was diluted with 0.22  $\mu\text{m}$ -filtered seawater (FSW) and the target cell types  
358 were identified microscopically based on morphology. Archeocytes are much larger  
359 than the other cells and possess a highly visible nucleolus. Choanocytes remain in intact  
360 choanocyte chambers after dissociation. Pinacocytes, unlike the other cell types, are  
361 translucent and maintain protruding cytoplasmic processes after dissociation. This  
362 approach avoided misidentification of dissociated cell types, but could not determine  
363 whether these cells are in the process of dividing or differentiating. Individual cells or  
364 choanocyte chambers were collected under an inverted microscope (Nikon Eclipse Ti  
365 microscope) using a micropipette mounted on micromanipulator (MN-4, Narishige)  
366 connected to CellTram Oil (Eppendorf) (Supplementary video 2), flash frozen and

367 stored at -80°C. All cells were frozen within 15 min of dissociation. Samples used in CEL-  
368 Seq2 were comprised of pools of either five to six archeocytes or pinacocytes, or a single  
369 choanocyte chamber (~40-60 cells) (Extended Data Table 1). Based on differences in  
370 cell size, we estimated that these pools have similar amounts of total RNA. Three  
371 pinacocyte, and five archeocyte and choanocyte samples were collected from each of  
372 three sponges (Supplementary File S2).

373

### 374 **CEL-Seq2 sample preparation, sequencing and analysis**

375 Samples were prepared according to the CEL-Seq2 protocol<sup>17</sup> and sequenced on two  
376 lanes of Illumina HiSeq2500 on rapid mode using HiSeq Rapid SBS v2 reagents  
377 (Illumina); CEL-Seq2 libraries were randomised in relation to cell type and source adult  
378 sponge in these two lanes. CEL-Seq2 reads were processed using a publicly available  
379 pipeline (<https://github.com/yanailab/CEL-Seq-pipeline>; see additional supplementary  
380 [data on Dryad: /CEL-Seq pipeline/](#)). Read counts were obtained from demultiplexed  
381 reads mapped to *A. queenslandica* Aqu2.1 gene models<sup>18</sup>. Samples with read counts less  
382 than 10<sup>6</sup> were removed and not included in subsequent analyses (Supplementary File  
383 S2). For the samples included in the final analysis, approximately 60% of the reads  
384 successfully mapped to the genome (Extended Data Table 1), as per other studies using  
385 CEL-Seq<sup>30</sup>.

386

### 387 **Analysis of differentially expressed genes**

388 The mapped read counts were analysed for differential gene expression using the  
389 bioconductor package DESeq2<sup>20,31</sup> ([see additional supplementary data on Dryad:](#)  
390 [/DESeq2/](#)). Genes that had read counts with a row sum of zero were removed. Principle  
391 component analyses (PCA) were performed on blind variance stabilising transformed



392 (vst) counts obtained using DESeq2 and were visualised using the ggplot2 package<sup>32</sup>.  
393 Pairwise comparisons were conducted between each of the three cell types to generate  
394 a differentially expressed gene (DEG) list for each cell type using a false discovery rate  
395 (FDR) < 0.05. Venn diagrams were generated using VENNY  
396 (<http://bioinfogp.cnb.csic.es/tools/venny>) to visualise and compare the list of DEGs  
397 between each cell type. Heat maps were generated using the R-packages pheatmap<sup>33</sup>  
398 and RColorBrewer<sup>34</sup> to visualise the expression patterns between the cell types using  
399 the vst transformed counts, which were scaled into z score values ranging from -1 (low  
400 expression) to 1 (high expression).

401 All protein coding genes were annotated using blastp (e-value cutoff = 1e-3) and  
402 InterProScan (default settings), which were merged in Blast2GO<sup>35,36</sup>. KEGG annotations  
403 were obtained using the online tool BlastKOALA<sup>37</sup> ([see additional supplementary data  
404 on Dryad: /KEGG annotation](#)). Pathway analyses were performed using the annotations  
405 on the KEGG Mapper - Reconstruct Pathway tool<sup>38</sup>. Complete DEG lists with BLAST2GO,  
406 InterPro, Pfam, and phylostrata ID can be found in Supplementary File S3, as well as  
407 KEGG pathway enrichments in Supplementary File S5.

408 To identify the genes that best explain differences among cell type transcriptomes,  
409 we adopted the multivariate sparse Partial Least Squares Discriminant Analysis (sPLS-  
410 DA)<sup>19</sup>, implemented in the mixOmics package<sup>39</sup> in R v3.3.1 ([see additional  
411 supplementary data on Dryad: /sPLS-DA/README.txt](#)). This is a supervised analysis  
412 that uses the sample information (cell type) to identify the most predictive genes for  
413 classifying the samples according to cell type. The optimised numbers of genes per  
414 component were obtained by training and correctly evaluating the performance of the  
415 predictive model using 5-fold cross-validation, repeated 100 times. A sample plot was  
416 used to visualise the similarities between samples for the final sPLS-DA model with

417 95% confidence ellipses using the plotIndiv function in R. A heat map was used to  
418 visualise relative expression levels of the selected gene models for the two components,  
419 using vst counts and the package pheatmap<sup>33</sup> in R. Venn diagrams were generated using  
420 VENNY to visualise and compare the DEGs generated by DESeq2 and sPLS-DA.

421

## 422 **Phylostratigraphy**

423 To estimate the evolutionary age of genes up-regulated in each cell type,  
424 phylostratigraphy analyses<sup>21</sup> were performed using blastp and an e-value cutoff of  
425 0.001 on a custom database containing 1,757 genomes and transcriptomes<sup>40</sup> that was  
426 modified to account for *A. queenslandica*'s phylogenetic position (i.e. all eumetazoan and  
427 bilaterian taxa were moved into the metazoan phylostratum, and three phylostrata –  
428 poriferan, demosponge and haplosclerid – were added to increase the representation of  
429 poriferan transcriptomes; Supplementary File S6, [see additional supplementary data on](#)  
430 [Dryad: /Phylostratigraphy annotations/](#)). Every gene model in *A. queenslandica* was  
431 blasted against each sequence in the database, and its age of gene origin was inferred  
432 based on the oldest blast hit relative to a predetermined phylogenetic tree ([see](#)  
433 [additional supplementary data on Dryad: /Phylostratigraphy annotations/](#)).

434 Phylostrata enrichments were performed using the Fisher's exact test<sup>41</sup> in the  
435 BioConductor package, GeneOverlap<sup>42</sup> in R, to identify significant differences in gene  
436 age of the cell type DEG lists relative to the genome ([see additional supplementary data](#)  
437 [on Dryad: /Fig.3b-d and /ED\\_Fig3\\_files](#)). Enrichment (log odds ratio value above 0) and  
438 under-representation (log odds ratio value below 0) of each phylostrata found in the  
439 cell type DEG lists relative to the genome, were visualised using the R-packages  
440 pheatmap<sup>33</sup> and RColorBrewer<sup>34</sup>.

441

## 442 **Orthology analyses**

443 Orthology analyses were performed using FastOrtho<sup>43</sup> from a custom 'all-vs-all' blastp  
444 database of coding sequences from the genomes of *Saccharomyces cerevisiae*<sup>44</sup>,  
445 *Arabidopsis thaliana*<sup>45</sup>, *Creolimax fragrantissima*<sup>12</sup>, *Sphaeroforma arctica*<sup>46</sup>, *Capsaspora*  
446 *owczarzaki*<sup>47</sup>, *Monosiga brevicollis*<sup>48</sup>, and *Salpingoeca rosetta*<sup>10</sup>, using the following  
447 configuration settings: pv\_cutoff = 1e-5; pi\_cutoff = 0.0; pmatch\_cutoff = 0.0;  
448 maximum\_weight = 316.0; inflation = 1.5; blast\_e = 1e-5 ([see additional supplementary](#)  
449 [data on Dryad](#): /FastOrtho/). FastOrtho classifies all of the genes present in each  
450 genome into orthology groups (orthogroups, OGs), which contain all orthologous and  
451 paralogous genes from each species. Genes that do not have any orthologues in other  
452 species or paralogues within the same genome were not included in any orthogroups.  
453 To compare the gene lists between species in all downstream analyses, species-specific  
454 gene names were changed to the common orthogroup identifier.

455 Orthology analyses between *A. queenslandica* and *S. rosetta*, *C. fragrantissima*, and *C.*  
456 *owczarzaki* cell types were performed using the cell type-specific DEG lists obtained  
457 from previous studies on *S. rosetta*<sup>10</sup>, *C. fragrantissima*<sup>12</sup>, and *C. owczarzaki*<sup>11</sup>. The  
458 BioConductor package, GeneOverlap<sup>42</sup>, was used to identify (1) the number overlapping  
459 OGs between species and cell type, and (2) the statistical significance of that overlap  
460 based on list size and total number of OGs ([see additional supplementary data on Dryad](#):  
461 /Fig.3e). This function provided the odds ratio between the OG lists, where the null  
462 hypothesis was no significant overlap (odds ratio value of 1 or smaller) and the  
463 alternative being a significant overlap detected between the lists (odds ratio value over  
464 1), as well as a p-value calculated for odds ratio values over 1.

465 To supplement phylostratigraphy analyses of *Amphimedon* cell-type specific gene  
466 lists (Fig. 3 and Extended Data Fig. 3), the BioConductor package, GeneOverlap<sup>42</sup> was

467 used to identify the number and percentage of orthogroups that are also present in the  
468 genomes of *Arabidopsis thaliana*, *Saccharomyces cerevisiae*, *Creolimax fragrantissima*,  
469 *Sphaeroforma arctica*, *Capsaspora owczarzaki*, *Monosiga brevicollis*, and *Salpingoeca*  
470 *rosetta* (Extended Data Fig. 4 and Extended data Fig. 5; [see additional supplementary](#)  
471 [data on Dryad](#): /ED\_Fig4 and ED\_Fig5)

472

### 473 **Classification of gene expression levels into quartiles**

474 In addition to differential gene expression analyses for *Amphimedon* transcriptomes, the  
475 relative gene expression levels for all cell types were assigned to one of four expression  
476 quartiles based on the number of reads that mapped to a given Aqu2.1 gene model  
477 (Extended data Fig. 3). All zero read counts were discarded and the mean expression  
478 value of the non-transformed normalised count values of all samples (from all cell  
479 types) was used to calculate the quartile values. These values (Q<sub>1</sub>: 2.30, Q<sub>2</sub>: 6.06, Q<sub>3</sub>:  
480 15.83) were used to classify the expression of all of genes in each cell type into four  
481 groups based on transcript abundance, ranging from lowest (Q1) to highest (Q4).

482 Phylostrata enrichments for the different quartile value thresholds were performed  
483 as described above for the cell type DEG lists; heat maps were generated using  
484 pheatmap<sup>33</sup> in R ([see additional supplementary data on Dryad](#): /ED\_Fig3\_files). All  
485 downstream analyses used the median value (Q<sub>2</sub>: 6.06) as a cut-off value to obtain a list  
486 of expressed genes. Orthology analyses using FastOrtho were performed as described  
487 above, and the percentage of genes with shared orthologous group (OG) in each gene  
488 list was calculated ([see additional supplementary data on Dryad](#): /ED\_Fig4\_files and  
489 ED\_Fig5\_files). In these analyses, exclusive lists refer to all of the regions in the Venn  
490 diagram being treated as a separate list (e.g. archeocyte only, common between  
491 archeocyte and choanocyte, common between archeocyte and pinacocyte, etc.), while

492 non-exclusive lists collapse all of the lists containing a given cell type into one list (e.g.  
493 archeocyte non-exclusive DEG list includes, archeocyte DEGs + (archeocyte + pinacocyte  
494 DEGs) + (archeocyte + choanocyte DEGs).

495

#### 496 **Identification and analysis of expressed *A. queenslandica* transcription factors**

497 A list of *A. queenslandica* transcription factors expressed in the three cell types was  
498 obtained using a number of independent methods. First, a non-conservative list of  
499 putative *A. queenslandica* transcription factors was obtained using the DNA-binding  
500 domain database (DBD: Transcription factor prediction database) and the Pfam IDs of  
501 sequence specific DNA-binding domain (DBD) families, which corresponds to known  
502 transcription factor families ([www.transcriptionfactor.org](http://www.transcriptionfactor.org)<sup>49</sup>). Second, we collated a list  
503 of annotated *A. queenslandica* transcription factors in the literature<sup>7,16,47,50-66</sup>  
504 (Supplementary File S8). Third, we compared these lists to an unpublished in-house  
505 database for *A. queenslandica* (Degnan *et al.* unpublished) and putative transcription  
506 factors identified by OrthoMCL. The final list of 173 expressed transcription factor  
507 genes used in this study were present in at least two of the three lists (Supplementary  
508 File S8).

509 The evolutionary age of each of the expressed transcription factors was first assigned  
510 based on the DBD contained in the gene model and then manually curated based  
511 primarily on literature (Supplementary File S8). From this, each TF was assigned as  
512 either originating in sponges after diverging from other animals (sponge-specific), in  
513 metazoans after they diverged from choanoflagellates (metazoan) or before metazoans  
514 diverged from choanoflagellates (premetazoan).

515

#### 516 **Analysis of juvenile cell fate and proliferation**

517 Larvae were collected as previously described<sup>67</sup>, left in FSW overnight and then placed  
518 in sterile 6-well plates with 10 ml of FSW for 1 hour in the dark with live coralline algae  
519 *Amphiroa fragilissima*. Postlarvae settled on *A. fragilissima* were removed using fine  
520 forceps (Dumont #5) and resettled on to round coverslips placed in a well with 2 ml  
521 FSW in a sterile 24-well plastic plate, with 3 postlarvae placed on each coverslip.  
522 Metamorphosis from resettled postlarvae to a functional juvenile takes approximately  
523 72 hours<sup>16,68</sup>. For all samples, FSW was changed daily until fixation.

524 The lipophilic cell tracker CM-DiI (Molecular Probes C7000) was used to label  
525 choanocyte chambers in juveniles as previously described<sup>16</sup>, with slight modifications in  
526 the concentration used and incubation times. *A. queenslandica* juveniles were incubated  
527 in 1  $\mu$ M CM-DiI in FSW for 30 minutes to 1 hour. This minimised the labelling of non-  
528 choanocyte cells. Despite this precaution, some non-choanocyte cells would be labelled  
529 in some individuals. Hence, all CM-DiI labelled juveniles were inspected by  
530 epifluorescence microscopy (Nikon Eclipse Ti microscope) immediately after CM-DiI  
531 was washed out, with juveniles detected with CM-DiI labelled cells outside of  
532 choanocyte chambers discarded from the study. Juveniles were allowed to develop for  
533 0, 2, 4, 6, 12 or 24 hours post-incubation (hpi) with CM-DiI, then washed in FSW three  
534 times for 5 minutes and fixed<sup>69</sup> without dehydration in ethanol. Fixed juveniles were  
535 washed three times in MOPST (1x MOPS buffer + 0.1% Tween). Nuclei were labelled  
536 with DAPI (1:1,000, Molecular Probes) for 30 minutes, washed in MOPST for 5 minutes  
537 and mounted using ProlongGold antifade reagent (Molecular Probes). All samples were  
538 observed using the ZEISS LSM 710 META confocal microscope, and image analysis was  
539 performed using the software ImageJ.

540 To visualise cell proliferation, the thymidine analogue EdU (Click-iT EdU AlexaFluor  
541 488 cell proliferation kit, Molecular Probes C10337) was used as previously

542 described<sup>16,26</sup>. To label S-phase nuclei, juveniles were incubated in FSW containing 200  
543  $\mu$ M EdU for 6 hours, washed in FSW and immediately fixed as described above.  
544 Fluorescent labelling of incorporated EdU was conducted according to the  
545 manufacturer's recommendations prior to DAPI labelling and mounting in ProLong Gold  
546 antifade reagent as described above.

547

548

## 549 **References (Methods)**

550

551 30 Levin, M. *et al.* The mid-developmental transition and the evolution of animal body  
552 plans. *Nature* **531**, 637-641 (2016).

553 31 Anders, S. & Huber, W. Differential expression analysis for sequence count data.  
554 *Genome Biol.* **11**, R106 (2010).

555 32 Wickham, H. *ggplot2: Elegant Graphics for Data Analysis* (Springer, 2009).

556 33 Kolde, R. Package 'pheatmap'. <https://cran.r-project.org/package=pheatmap>  
557 (2012).

558 34 Neuwirth, E. Package 'RColorBrewer'. [https://cran.r-](https://cran.r-project.org/package=RColorBrewer)  
559 [project.org/package=RColorBrewer](https://cran.r-project.org/package=RColorBrewer) (2011).

560 35 Conesa, A. *et al.* Blast2GO: a universal tool for annotation, visualization and analysis  
561 in functional genomics research. *Bioinformatics* **21**, 3674-3676 (2005).

562 36 Götz, S. *et al.* High-throughput functional annotation and data mining with the  
563 Blast2GO suite. *Nucleic Acids Res.* **36**, 3420-3435 (2008).

564 37 Kanehisa, M., Sato, Y. & Morishima, K. BlastKOALA and GhostKOALA: KEGG tools for  
565 functional characterization of genome and metagenome sequences. *J. Mol. Biol.* **428**,  
566 726-731 (2016).

- 567 38 Kanehisa, M., Sato, Y., Kawashima, M., Furumichi, M. & Tanabe, M. KEGG as a  
568 reference resource for gene and protein annotation. *Nucleic Acids Res.* **44**, D457-  
569 D462 (2015).
- 570 39 Rohart, F., Gautier, B., Singh, A. & Le Cao, K.-A. mixOmics: an R package for 'omics  
571 feature selection and multiple data integration. *PLoS Comput. Biol.* **13**, e1005752  
572 (2017).
- 573 40 Aguilera, F., McDougall, C. & Degnan, B. M. Co-Option and *de novo* gene evolution  
574 underlie molluscan shell diversity. *Mol. Biol. Evol.* **34**, 779-792 (2017).
- 575 41 Domazet-Lošo, T., Brajković, J. & Tautz, D. A phylostratigraphy approach to uncover  
576 the genomic history of major adaptations in metazoan lineages. *Trends Genet.* **23**,  
577 533-539 (2007).
- 578 42 Shen, L. GeneOverlap: An R package to test and visualize gene overlaps. (2014).
- 579 43 Wattam, A. R. *et al.* PATRIC, the bacterial bioinformatics database and analysis  
580 resource. *Nucleic Acids Res.* **42**, D581-591 (2014).
- 581 44 Yates, A. *et al.* Ensembl 2016. *Nucleic Acids Res.* **44**, D710-D716 (2016).
- 582 45 The Arabidopsis Genome Initiative. Analysis of the genome sequence of the  
583 flowering plant *Arabidopsis thaliana*. *Nature* **408**, 796-815 (2000).
- 584 46 Ruiz-Trillo, I., Lane, C. E., Archibald, J. M. & Roger, A. J. Insights into the evolutionary  
585 origin and genome architecture of the unicellular opisthokonts *Capsaspora*  
586 *owczarzaki* and *Sphaeroforma arctica*. *J. Eukaryot. Microbiol.* **53**, 379-384 (2006).
- 587 47 Suga, H. *et al.* The *Capsaspora* genome reveals a complex unicellular prehistory of  
588 animals. *Nat. Commun.* **4**, 2325 (2013).
- 589 48 King, N. *et al.* The genome of the choanoflagellate *Monosiga brevicollis* and the origin  
590 of metazoans. *Nature* **451**, 783-788 (2008).



- 591 49 Wilson, D., Charoensawan, V., Kummerfeld, S. K. & Teichmann, S. A. DBD -  
592 taxonomically broad transcription factor predictions: new content and  
593 functionality. *Nucleic Acids Res.* **36**, D88-92 (2008).
- 594 50 Babonis, L. S. & Martindale, M. Q. Phylogenetic evidence for the modular evolution  
595 of metazoan signalling pathways. *Philos. Trans. R. Soc. Lond. B. Biol. Sci.* **372**,  
596 20150477 (2017).
- 597 51 Srivastava, M. *et al.* Early evolution of the LIM homeobox gene family. *BMC Biol.* **8**, 4  
598 (2010).
- 599 52 Larroux, C. *et al.* Genesis and expansion of metazoan transcription factor gene  
600 classes. *Mol. Biol. Evol.* **25**, 980-996 (2008).
- 601 53 Larroux, C. *et al.* Developmental expression of transcription factor genes in a  
602 demosponge: insights into the origin of metazoan multicellularity. *Evol. Dev.* **8**, 150-  
603 173 (2006).
- 604 54 Shimeld, S. M., Degnan, B. & Luke, G. N. Evolutionary genomics of the Fox genes:  
605 origin of gene families and the ancestry of gene clusters. *Genomics* **95**, 256-260  
606 (2010).
- 607 55 Layden, M. J., Meyer, N. P., Pang, K., Seaver, E. C. & Martindale, M. Q. Expression and  
608 phylogenetic analysis of the *zic* gene family in the evolution and development of  
609 metazoans. *EvoDevo* **1**, 12 (2010).
- 610 56 Presnell, J. S., Schnitzler, C. E. & Browne, W. E. KLF/SP transcription factor family  
611 evolution: Expansion, diversification, and innovation in eukaryotes. *Genome Biol.*  
612 *Evol.* **7**, 2289-2309 (2015).
- 613 57 Mukhopadhyay, S. & Jackson, P. K. The tubby family proteins. *Genome Biol.* **12**, 225  
614 (2011).

- 615 58 Larroux, C. *et al.* The NK homeobox gene cluster predates the origin of Hox genes.  
616 *Curr. Biol.* **17**, 706-710 (2007).
- 617 59 Wang, L., Tang, Y., Cole, P. A. & Marmorstein, R. Structure and chemistry of the  
618 p300/CBP and Rtt109 histone acetyltransferases: Implications for histone  
619 acetyltransferase evolution and function. *Curr. Opin. Struct. Biol.* **18**, 741-747  
620 (2008).
- 621 60 Petroni, K. *et al.* The promiscuous life of plant NUCLEAR FACTOR Y transcription  
622 factors. *Plant Cell* **24**, 4777-4792 (2012).
- 623 61 Morrison, A. J. & Shen, X. Chromatin remodelling beyond transcription: the INO80  
624 and SWR1 complexes. *Nat. Rev. Mol. Cell Biol.* **10**, 373-384 (2009).
- 625 62 Jones, M. H., Hamana, N., Nezu, J. & Shimane, M. A novel family of bromodomain  
626 genes. *Genomics* **63**, 40-45 (2000).
- 627 63 Song, W., Solimeo, H., Rupert, R. A., Yadav, N. S. & Zhu, Q. Functional dissection of a  
628 Rice Dr1/DrAp1 transcriptional repression complex. *Plant Cell* **14**, 181-195 (2002).
- 629 64 Matheos, D. P., Kingsbury, T. J., Ahsan, U. S. & Cunningham, K. W. Tcn1p/Crz1p, a  
630 calcineurin-dependent transcription factor that differentially regulates gene  
631 expression in *Saccharomyces cerevisiae*. *Genes Dev.* **11**, 3445-3458 (1997).
- 632 65 Rivera, A. S. *et al.* Gene duplication and the origins of morphological complexity in  
633 pancrustacean eyes, a genomic approach. *BMC Evol. Biol.* **10**, 123, (2010).
- 634 66 Romanovskaya, E. V. *et al.* Transcription factors of the NF1 family: Possible  
635 mechanisms of inducible gene expression in the evolutionary lineage of  
636 multicellular animals. *J. Evol. Biochem. Physiol.* **53**, 85-92 (2017).
- 637 67 Leys, S. P. *et al.* Isolation of *Amphimedon* developmental material. *Cold Spring Harb.*  
638 *Protoc.* **3**, 5095 (2008).

639 68 Degnan, B. M. *et al.* Porifera. *Evolutionary Developmental Biology of Invertebrates*  
640 *vol.1* (Springer, 2015).

641 69 Larroux, C. *et al.* Whole-mount in situ hybridization in *Amphimedon*. *Cold Spring*  
642 *Harb. Protoc.* **3**, 5096 (2008).

643

644

645

#### 646 **Extended Data Figure Legends**

647

#### 648 **Extended Data Figure 1: Sparse partial least squares discriminant analysis (sPLS-** 649 **DA) of *Amphimedon queenslandica* choanocyte, archeocyte and pinacocyte** 650 **transcriptomes.**

651 A supervised multivariate analysis, sPLS-DA, identified the gene models that best  
652 characterise differences in choanocytes (blue), archeocytes (red) and pinacocytes  
653 (green). **a**, Sample plot for the optimal number of gene models that discriminate cell  
654 types on the first two components; ellipses indicate 95% confidence intervals. **b, c**,  
655 Hierarchically-clustered heat maps show the expression of (b) the 110 gene models  
656 selected for the first component, and (c) the 98 gene models and 2 long non-coding  
657 RNAs selected for the second component, which accounted for 15% and 5% of  
658 explained variance, respectively. **d, e**, Venn diagrams summarise the significantly  
659 differentially expressed genes identified by the DESeq2 analyses, for each cell type, and  
660 the sPLS-DA on (d) the first and (e) the second sPLS-DA component. Percentages are of  
661 the total number of differentially expressed genes identified from all analyses.

662

663 **Extended Data Figure 2: Percentage of KEGG cellular processes and**  
664 **environmental information processing (i.e. cell signalling) genes present in each**  
665 **cell type, corresponding to the number of components making up each KEGG**  
666 **category identified.**

667 **a**, Cellular processes genes. **b**, Environmental information processing (i.e. cell  
668 signalling) genes.

669

670 **Extended Data Figure 3: Evolutionary age of genes expressed in *Amphimedon***  
671 ***queenslandica* choanocytes, archeocytes and pinacocytes using different**  
672 **expression thresholds.**

673 **a-e**, Phylostratigraphic enrichment of genes expressed in each cell type (Ar, archeocyte;  
674 Ch, choanocyte; Pi, pinacocyte; ArCh, archeocyte + choanocyte; ArPi, archeocyte +  
675 pinacocyte; ChPi, choanocyte + pinacocyte; ALL, all three cell types combined) at  
676 different expression thresholds. Expressed genes are parsed into quartiles based on  
677 transcript abundance in each of the cell types. Quartile 1 (Q1) includes the least  
678 abundant transcripts and Q4 the most abundant. **a**, Phylostratigraphy enrichment of all  
679 genes expressed in each of the cell types (i.e. Q1-Q4). **b**, Phylostratigraphy enrichment  
680 of genes expressed in the top three quartiles (i.e. excluding Q1). **c**, Phylostratigraphy  
681 enrichment of genes expressed in the top 50% (i.e. Q3 and Q4). **d**, Phylostratigraphy  
682 enrichment of the most highly expressed genes (i.e. Q4). **e**, For comparison, the  
683 evolutionary age of differentially expressed genes identified using differential  
684 expression analysis, DESeq2. Heat maps indicate enrichment (log odds ratio) of  
685 phylostrata contained in each gene list in comparison to the *A. queenslandica* genome.  
686 Asterisks mark significant ( $p < 0.05$ ) enrichment. The heat maps on the far right are  
687 collapsed versions of the heat maps on the left, where the premetazoan category

688 contains phylostrata from cellular to holozoan, and the poriferan category contains  
689 phylostrata from poriferan to *A. queenslandica*. To the left of each heat map is a Venn  
690 diagram, showing the number of genes in each cell type and sets of cell types. Grey  
691 boxes on the heat map indicate that there were no genes in that particular gene list  
692 characterised by the given phylostrata. **f**, Pairwise comparison illustrating the number  
693 of overlapping genes for each of the quartiles between the three cell types. The numbers  
694 in the cells are the number of genes common between two cell types (e.g. there are  
695 1569 expressed genes in common between Q2 in choanocytes and Q3 in archeocytes).  
696 NE, not expressed. **g**, The percentage of differentially up-regulated genes identified in  
697 each of the cell types using DESeq2 in the four quartiles.

698

699 **Extended Data Figure 4: Orthologues shared between cell type-specific gene lists**  
700 **and non-metazoan eukaryotes.**

701 Heat map showing the percentage of *A. queenslandica* genes with orthogroups (OGs)  
702 shared with select eukaryotes. **a**, Percentage of genes with OGs shared between up-  
703 regulated and total expressed genes from non-exclusive lists (i.e. all genes expressed in  
704 each of the three cell types, not excluding genes that overlap between any two cell  
705 types). **b**, Percentage of genes with OGs shared between DEG and total expressed genes  
706 - exclusive lists (i.e. genes uniquely up-regulated or expressed in that cell type).

707

708 **Extended Data Figure 5: Orthologues found in *Salpingoeca rosetta*, *Capsaspora***  
709 ***owczarzaki* and *Creolimax fragrantissima* life cycle stages, shared with *A.***  
710 ***queenslandica* cell type transcriptomes and eukaryotic genomes.**

711 **a**, The percent and number (in parentheses) of differentially expressed OGs found in  
712 *Salpingoeca rosetta*, *Capsaspora owczarzaki* and *Creolimax fragrantissima* life cycle

713 stages that are shared with *Amphimedon queenslandica* cell types. The numbers in  
714 parentheses alongside the unicellular holozoan cell states and sponge cell type names is  
715 the total number of OGs differentially expressed in that specific gene list. **b**, A heatmap  
716 showing the percentage of OGs shared between genes differentially expressed in  
717 *Salpingoeca rosetta*, *Capsaspora owczarzaki* and *Creolimax fragrantissima* life cycle  
718 stages, and genes present in other eukaryotic genomes.

719

720 **Extended Data Figure 6: Heat map of transcription factor genes differentially**  
721 **expressed in choanocytes, archeocytes and pinacocytes.**

722 94 transcription factor genes that are differentially expressed in *A. queenslandica* cell  
723 types are classified based on phylostratum: premetazoan (light grey); metazoan (dark  
724 grey; and poriferan (black). **a**, Heat map of expression levels in the three cell types  
725 combining all analysed CEL-Seq2 data. Gene names, families (in parentheses) and  
726 phylostrata shading are shown on the right. **b**, Heat map of expression levels of all CEL-  
727 Seq2 samples. Rows in b correspond to the rows and genes in a. **c**, Venn diagram  
728 summary of differentially up-regulated transcription factor genes between the three cell  
729 types using DESeq2. Percentages are of the total transcription factor genes differentially  
730 up-regulated in all cell types. **d**, Bar graph of the number and distribution of  
731 transcription factor genes based on evolutionary age in the three cell types.

732

733 **Extended Data Figure 7: Analysis of premetazoan transcription factors in**  
734 ***Amphimedon* cells and unicellular holozoan cell states.**

735 **a**, The number and percentage of premetazoan transcription factor orthologues that are  
736 present in the genomes of *Salpingoeca rosetta*, *Capsaspora owczarzaki* and *Creolimax*  
737 *fragrantissima*. Percentages are based on the 43 premetazoan genes differentially

738 expressed in the *A. queenslandica* cell types (Extended Data Fig. 5). The number of  
739 transcription factor orthologues in the genome is listed above the bar. The orange bar  
740 depicts the percent and number of unicellular holozoan premetazoan transcription  
741 factor orthologues that are significantly differentially up-regulated in at least one cell  
742 state. **b**, The 15 premetazoan transcription factor orthology groups (listed along the  
743 top) that are significantly up-regulated in at least one *Amphimedon* cell type and one  
744 unicellular holozoan cell state. Dots correspond to the cell types and states this occurs.  
745 Black dots, orthology group with one gene member; grey dots, orthology group  
746 comprised of two or more paralogues (see Supplementary File S8 for details).

747

748 **Extended Data Figure 8: Choanocyte dedifferentiation into an archeocyte does not**  
749 **require cell division.**

750 **a, b**, 4 day old juveniles 6 hours after CM-DiI and EdU labelling. **a**, CM-DiI labelled  
751 archeocytes with EdU incorporation (arrows) found near choanocyte chambers. **b**,  
752 Labelled archeocytes without EdU incorporation (arrowheads), indicating  
753 dedifferentiation from choanocytes without cell division. Scale bars: 10  $\mu$ m.  
754 **c, d**, Choanocyte-derived archeocytes are capable of generating new choanocyte  
755 chambers. **c**, 4 day old juvenile 6 hours after CM-DiI and EdU labelling. Early choanocyte  
756 chamber (dotted line) completely labelled with CM-DiI and EdU, indicating CM-DiI  
757 labelled archeocytes, with large nuclei, are forming this chamber. The absence of cilia  
758 and space at the center of this structure indicates it is not yet a functional choanocyte  
759 chamber. **d**, 4 day old juvenile 12 hours after CM-DiI and 6 hours after EdU labelling.  
760 Early choanocyte chamber (dotted line) with multiple EdU labelled cells, with both CM-  
761 DiI labelled choanocytes (arrowheads) and non-CM-DiI labelled choanocytes (arrows)

762 indicate multiple cell lineages contributing to the formation of this chamber. Scale bars:

763 **a-d**, 10  $\mu\text{m}$ .

764

765

## 766 **Supplementary Video Legends**

767

### 768 **Supplementary Video 1: Time-lapse video of a 4 day old juvenile *Amphimedon***

769 ***queeslandica*.**

770 This 10 second video captures 20 minutes of cell behavior on the outer edge of the

771 juvenile. Annotated are (i) a choanocyte chamber (cc) comprising of multiple tethered

772 choanocytes, (ii) three migrating archeocytes (ar) – there are multiple other

773 archeocytes in this video, and (iii) a pinacocyte (pi), which comes in and out of focus

774 and is characterised by a thin, transparent cytoplasm with small refractive vesicles.

775 Scale bar, 10  $\mu\text{m}$ .

776

### 777 **Supplementary Video 2: Capture and washing of a dissociated archeocyte.**

778 All cells and choanocyte chambers used in this study were fixed or frozen in less than 15

779 minutes after dissociation from the intact sponge.

780

### 781 **Supplementary Video 3: Time-lapse video of choanocytes transdifferentiating and**

782 **evacuating chambers in 4 day old juvenile *Amphimedon queeslandica*.**

783 Matching 8-second videos captures 120 min of CM-DiI labelled choanocytes (left, red;

784 right, white), which are initially located in distinct chambers (arrows on four

785 chambers), undergoing transdifferentiation and migrating from the chambers. At the

786 end of the video, none of the CM-DiI labelled chambers are recognisable. Note that many



787 cells vacating the choanocyte chambers are larger, consistent with choanocytes

788 dedifferentiating into larger archeocytes. Scale bar, 40  $\mu$ m.

789

790

## 791 **Supplementary Files**

792

793 **Supplementary File S1. The counting report of the cell type specific CEL-Seq2**

794 **samples**

795

796 **Supplementary File S2. Table summarising the details and the statistics of the**

797 **demultiplexing and mapping steps for the cell type specific CEL-Seq2 samples**

798

799 **Supplementary File S3. Table of differentially expressed gene lists from DESeq2**

800 **with BLAST2GO annotations and phylostrata ID**

801

802 **Supplementary File S4. Table of differentially expressed gene lists from sPLS-DA**

803 **with BLAST2GO and KEGG annotations and phylostrata ID**

804

805 **Supplementary File S5. Table of KEGG enrichment analysis results on**


806 **differentially expressed gene lists from DESeq2**

807 This spreadsheet contains the output of KEGG enrichment analyses performed on each

808 cell type DEG list. The first sheet contains percentage values of genes/components

809 identified in the DEG lists relative to the *A. queenslandica* genome.


810

811 **Supplementary File S6. Table of the phylostrata enrichment of the differentially**  
812 **expressed gene lists from DESeq2** 

813

814 **Supplementary File S7. Table of cell-type gene lists and transcription factor lists**  
815 **from the quartile expression analyses**

816

817 **Supplementary File S8. Table of transcription factor genes expressed in the three**  
818 **cell types and in the differentially expressed gene lists from DESeq2** 

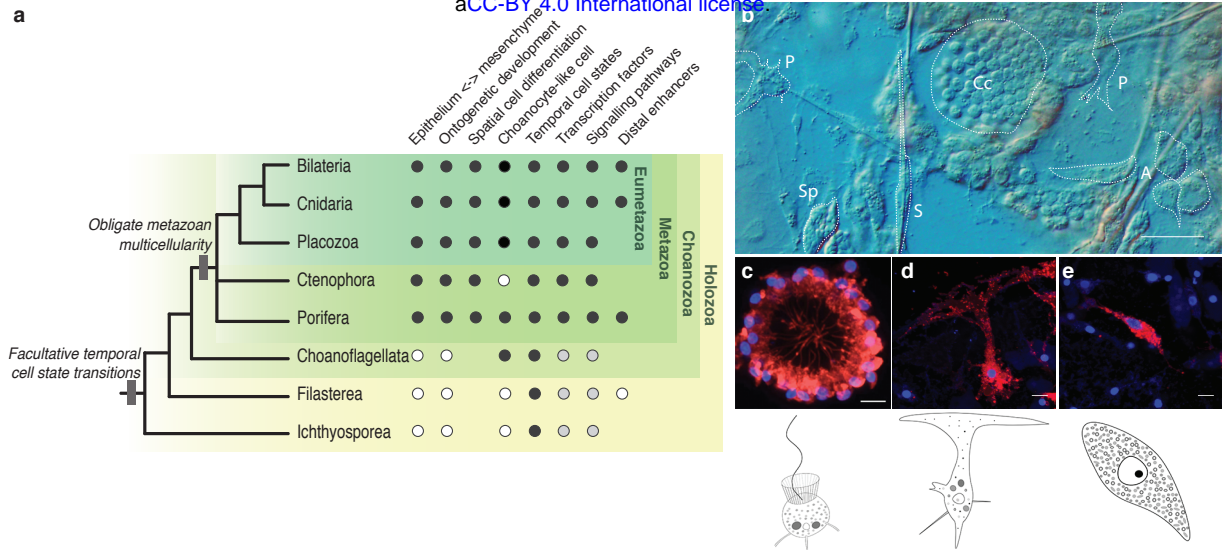


Fig. 1

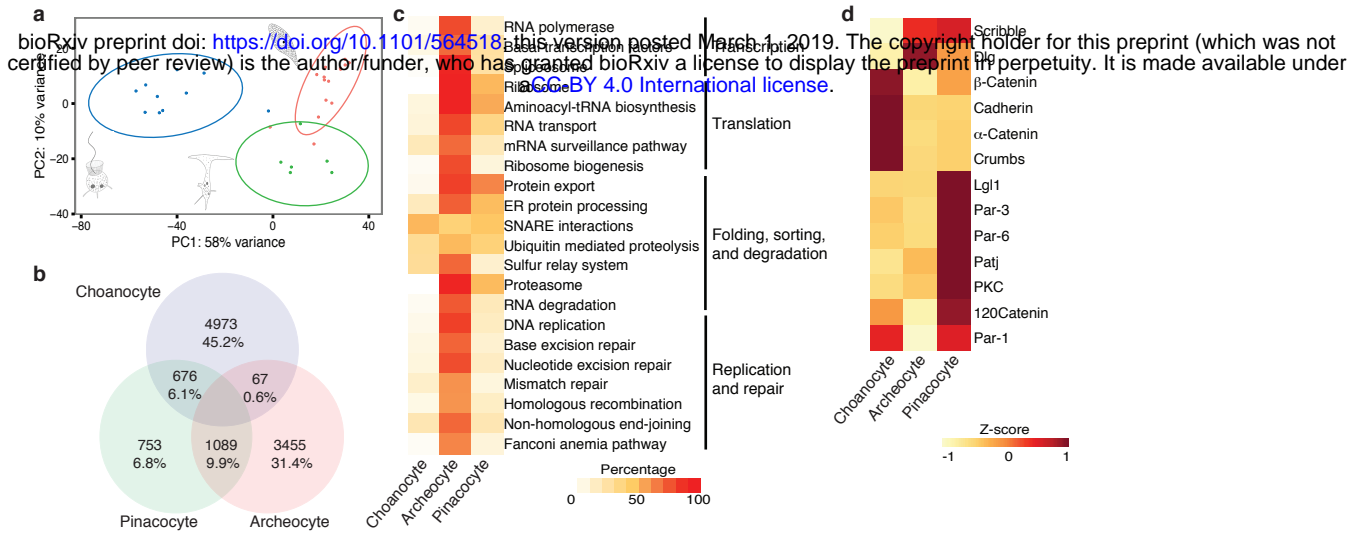


Fig. 2

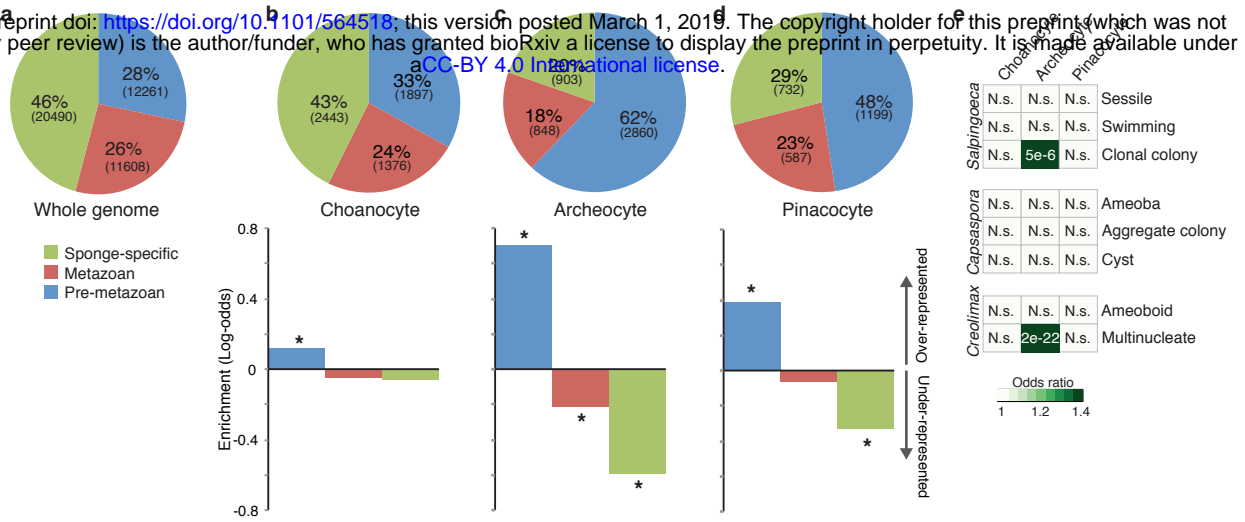


Fig. 3

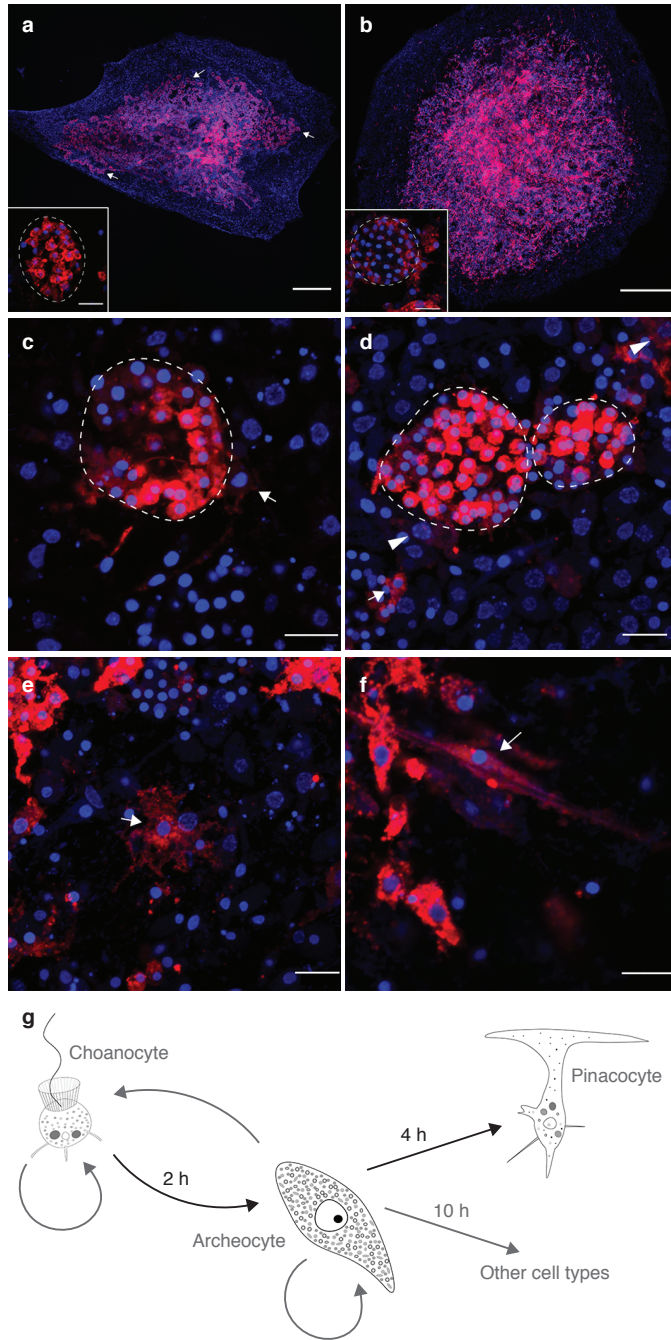
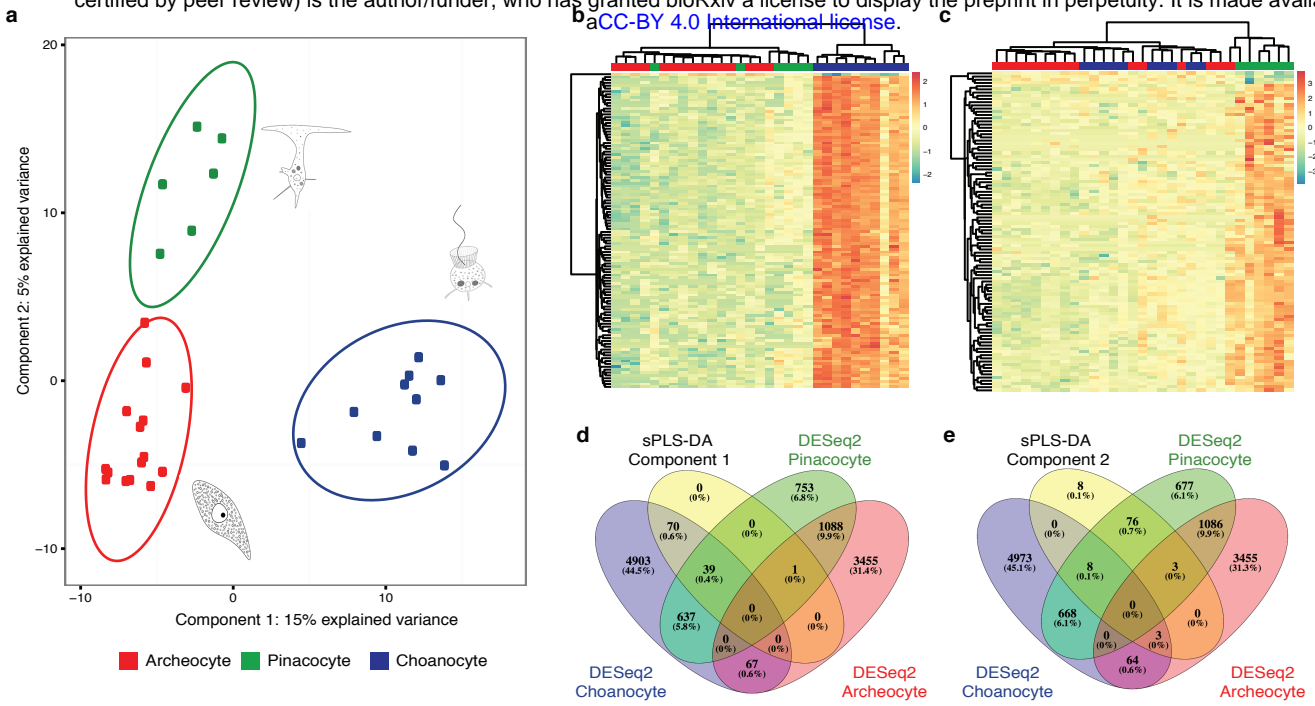


Fig. 4

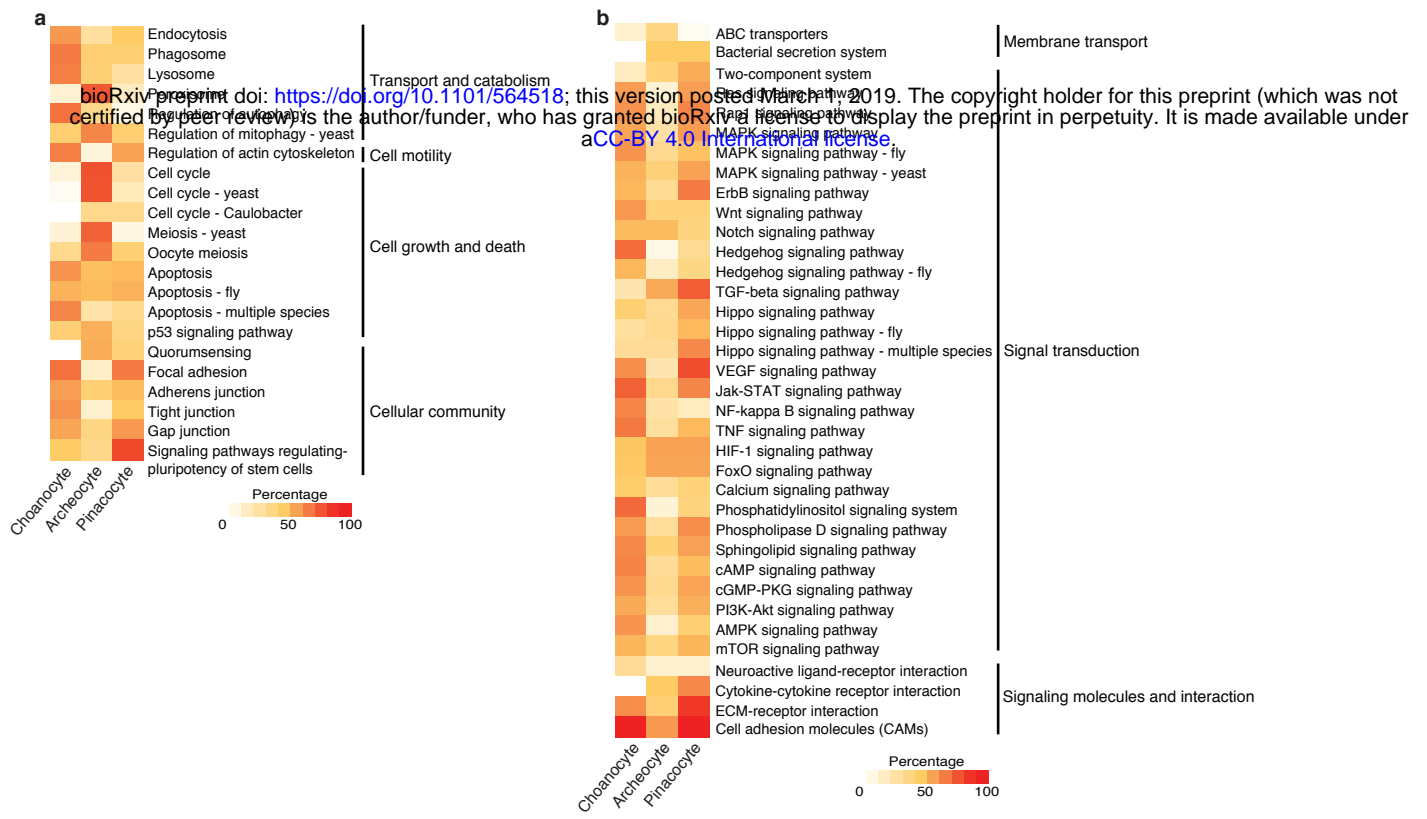
**Extended Data Table 1 | Summary of CEL-Seq2 samples used in this study**

Sample	Cell type	Individual	No. cells sequenced	No. reads	Percent reads mapped	
1	Archeocyte	A	5	1098454	21.4	
2			5	10411743	67.6	
3			5	5699424	60.3	
4			6	6759553	72.6	
5			5	5673223	64.7	
6		B	5	14421299	65.5	
7			5	9427170	64.0	
8			5	8208828	65.3	
9			5	13012311	71.1	
10			5	11700365	71.7	
11	C	5	25125367	69.8		
12		5	15458602	69.7		
13		6	16070906	70.6		
14		5	20190551	71.0		
15		6	22096837	71.7		
16	Choanocyte	A	single chamber (40-60 cells)	9657992	49.2	
17			single chamber (40-60 cells)	3864298	47.2	
18			single chamber (40-60 cells)	7081396	59.7	
19			B	single chamber (40-60 cells)	5177297	61.9
20				single chamber (40-60 cells)	6031263	64.9
21		C	single chamber (40-60 cells)	14879156	62.4	
22			single chamber (40-60 cells)	12775312	67.0	
23			single chamber (40-60 cells)	10569223	66.7	
24			single chamber (40-60 cells)	17488774	64.1	
25			single chamber (40-60 cells)	18808800	67.1	
26	Pinacocyte	A	5	19146512	67.6	
27			5	12081597	69.6	
28			5	10798371	67.6	
29		B	6	2906098	58.1	
30			C	5	13792427	60.0
31		5		5184625	66.0	

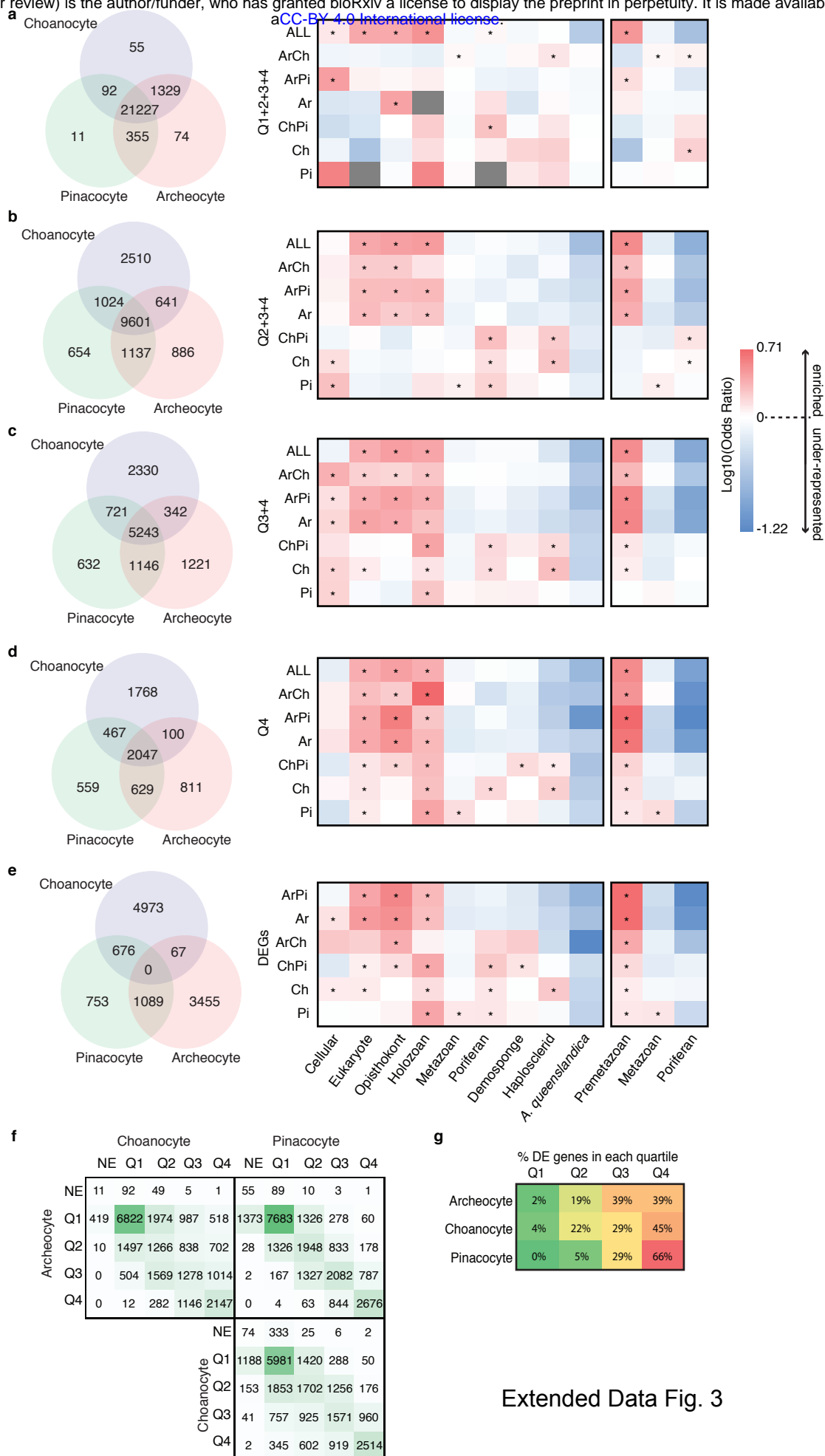


Extended Data Fig. 1

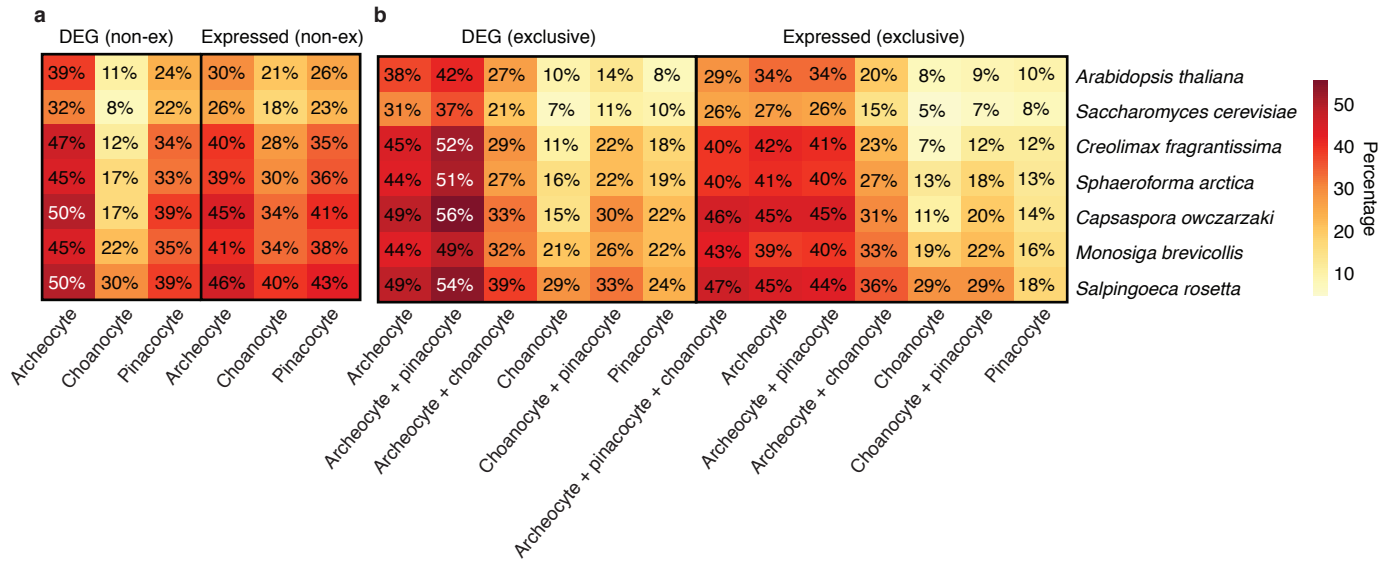




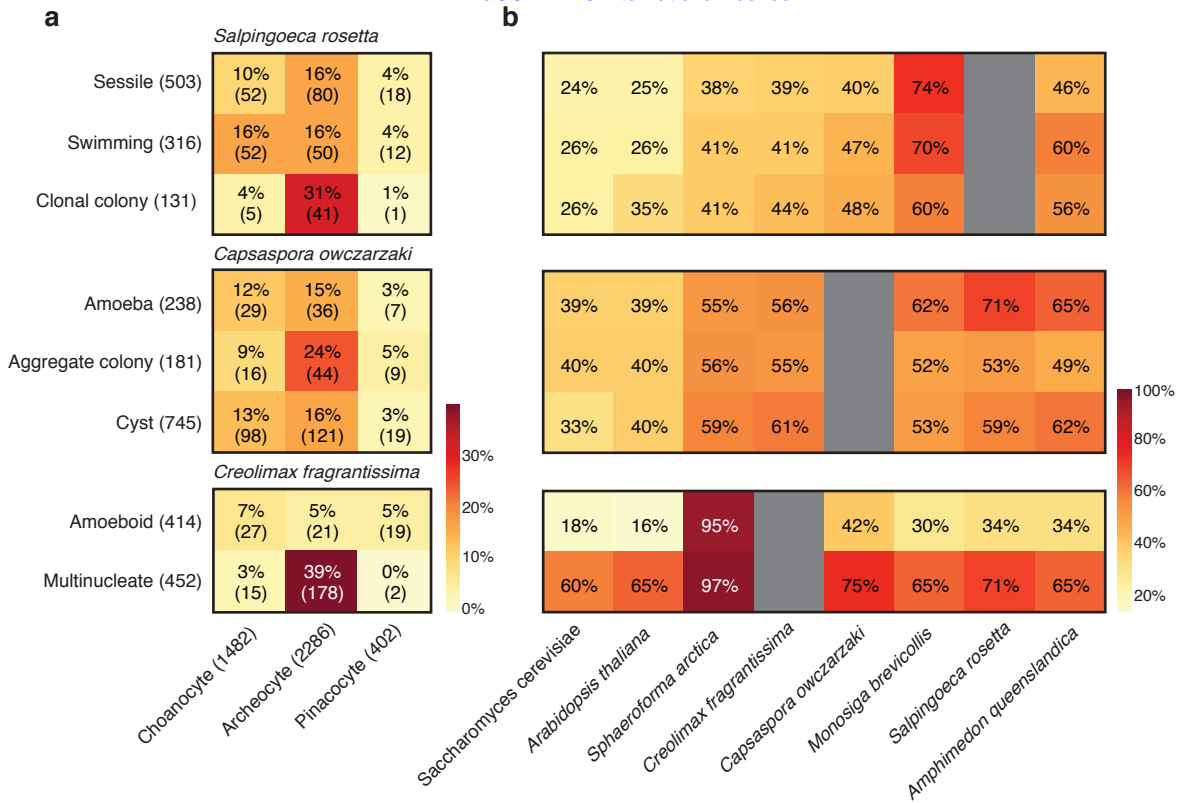
Extended Data Fig. 2



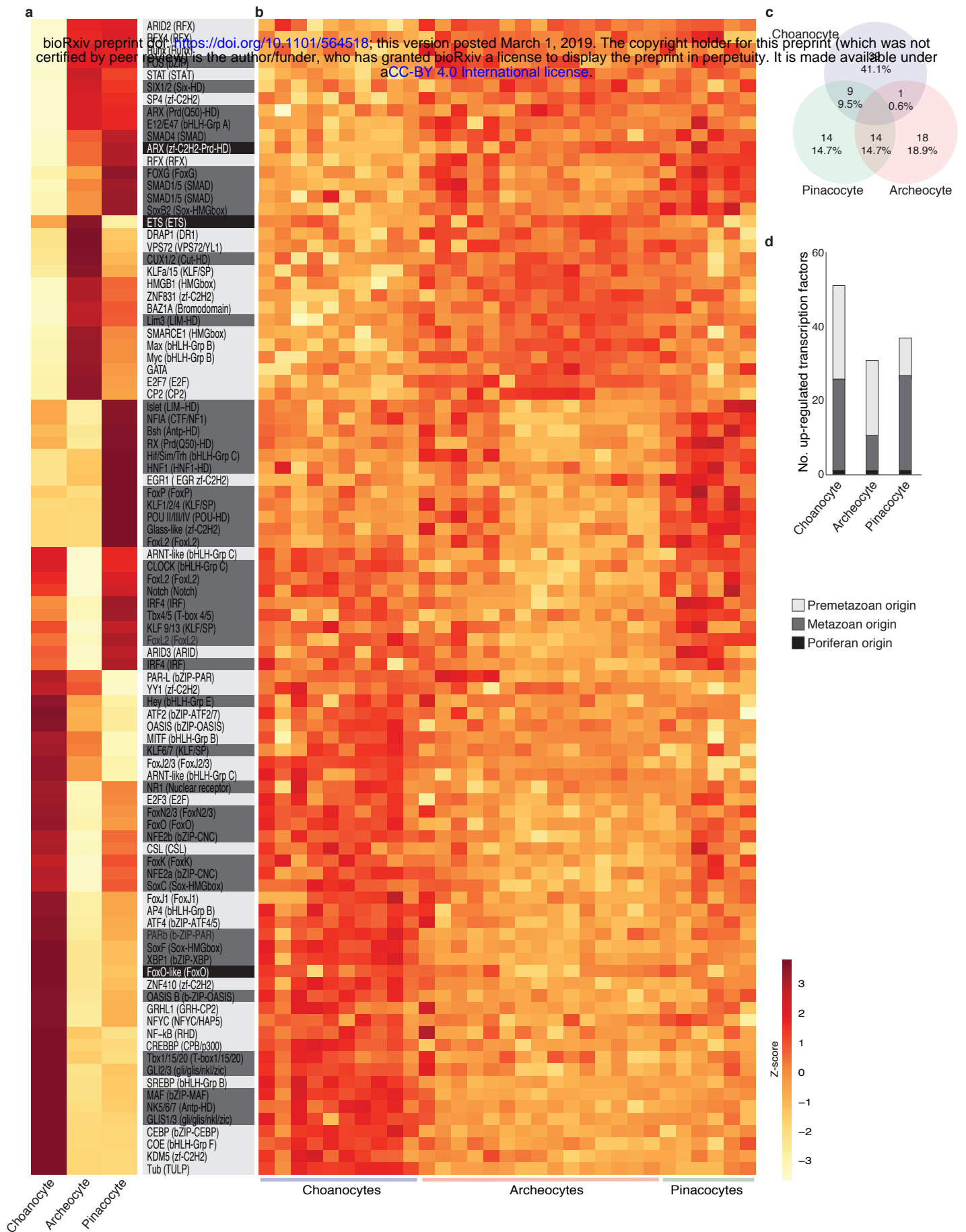
Extended Data Fig. 3



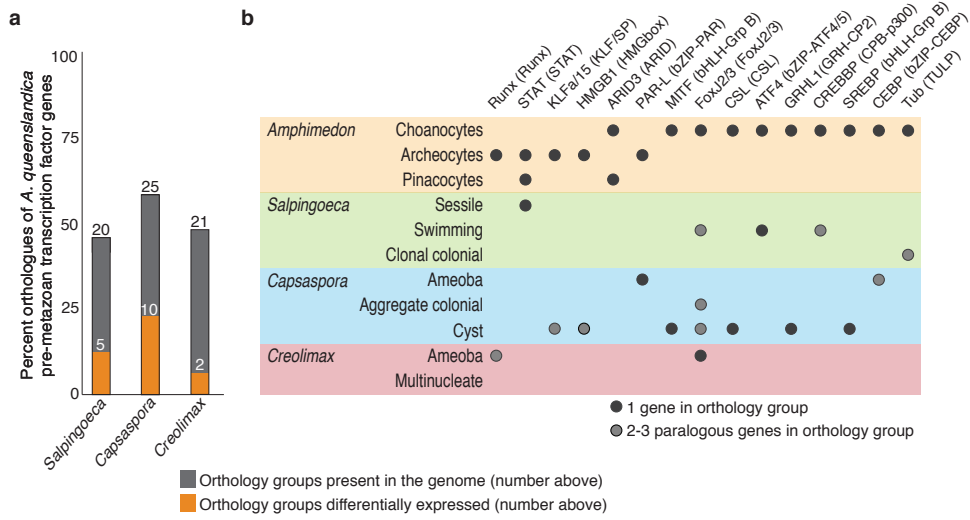
Extended Data Fig. 4



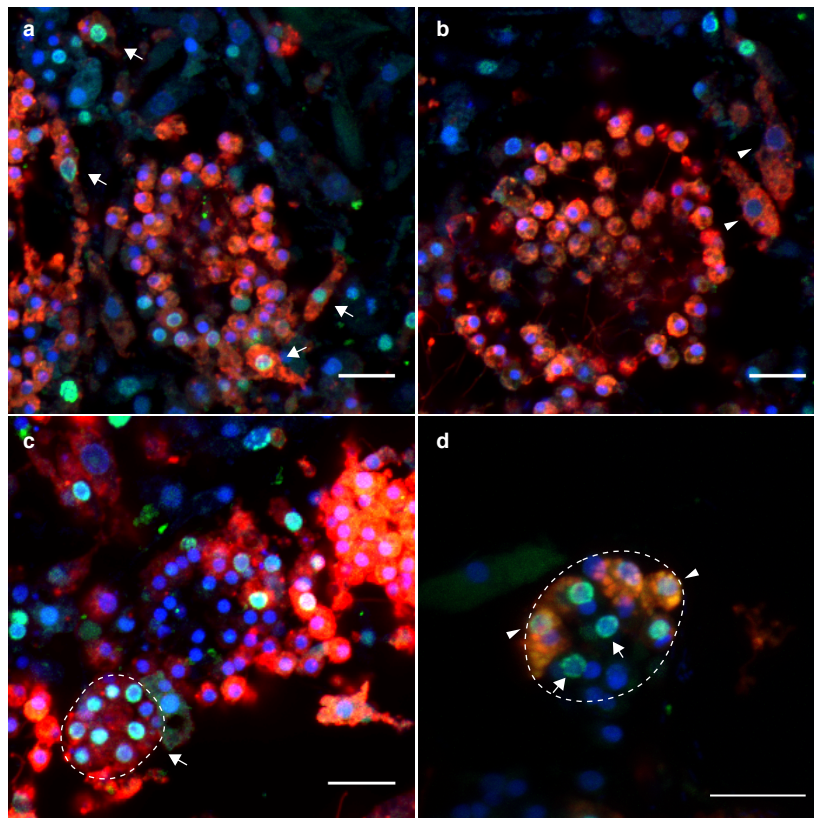
Extended Data Fig. 5



Extended Data Fig. 6



Extended Data Fig. 7



Extended Data Fig. 8